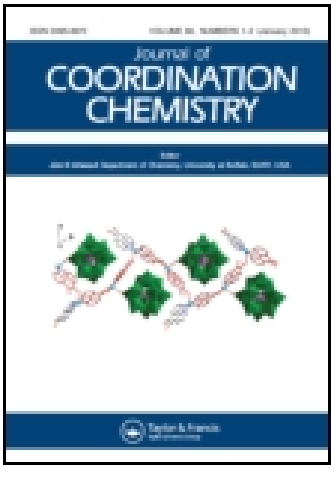

Journal of Coordination Chemistry
Publication details, including instructions for authors and subscription information:
http://www.tandfonline.com/loi/gcoo20

Structural diversity of a series of chlorocadmate(II) and chlorocuprate(II) complexes based on benzylamine and its N-methylated derivatives

Yu Jin[a], Chun-Hua Yu[a] & Wen Zhang[a]
[a] Ordered Matter Science Research Center, Southeast University, Nanjing, China

Accepted author version posted online: 02 Apr 2014.Published online: 29 Apr 2014.

To cite this article: Yu Jin, Chun-Hua Yu & Wen Zhang (2014) Structural diversity of a series of chlorocadmate(II) and chlorocuprate(II) complexes based on benzylamine and its N-methylated derivatives, Journal of Coordination Chemistry, 67:7, 1156-1173, DOI: 10.1080/00958972.2014.909589

To link to this article: http://dx.doi.org/10.1080/00958972.2014.909589

Journal of Coordination Chemistry, 2014
Vol. 67, No. 7, 1156–1173, http://dx.doi.org/10.1080/00958972.2014.909589

Structural diversity of a series of chlorocadmate(II) and chlorocuprate(II) complexes based on benzylamine and its *N*-methylated derivatives

YU JIN, CHUN-HUA YU and WEN ZHANG*

Ordered Matter Science Research Center, Southeast University, Nanjing, China

(*Received 31 October 2013; accepted 12 March 2014*)

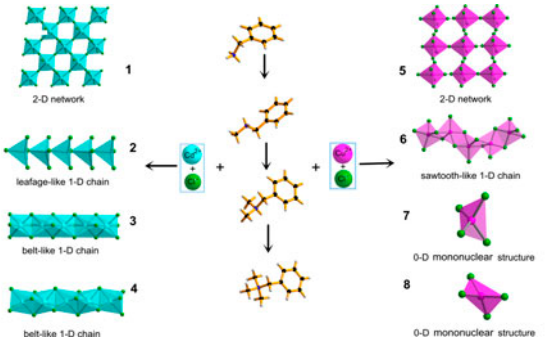

Protonated benzylamine and its *N*-methylated derivatives, $[C_6H_5CH_2NH_{3-n}(CH_3)_n]^+$ ($n = 0-3$), have been adopted as cations in chlorocadmate(II) and chlorocuprate(II) complexes, showing inorganic–organic hybrid architectures. For the Cd(II) compounds, the anionic structures vary from perovskite-type layers ($n = 0$) to chains ($n = 1–3$). For Cu(II) compounds, the anionic structures range from perovskite-type layers ($n = 0$), chains ($n = 1$) to mononuclear species ($n = 2–3$). Coordination geometries of the metal ions and intermolecular interactions have been analyzed. Their dielectric properties have been measured.

Keywords: Cadmium; Copper; Benzylamine; Hydrogen bonds; Crystal structure

1. Introduction

It is a central topic in crystal engineering to understand and control intermolecular interactions among the building blocks so as to correlate structures and desired properties of crystalline molecule-based materials [1, 2]. Successful manipulation of these interactions

*Corresponding author. Email: zhangwen@seu.edu.cn

enables people to produce materials with technologically useful properties, such as ferroelectricity [3, 4]. For molecule-based crystals, crystal packing is determined not only by the shapes of building blocks but also, to a large extent, by non-covalent interactions such as hydrogen bonds, van der Waals interactions, and ionic bonds [5–9].

Herein, we choose protonated benzylamine and its *N*-methylated derivatives, $[C_6H_5CH_2NH_{3-n}(CH_3)_n]^+$ ($n = 0$, L^1; $n = 1$, L^2; $n = 2$, L^3; $n = 3$, L^4), as organic cations to explore their effects on structures of the inorganic–organic hybrid compounds based on Cd (II) and Cu(II) chlorides. The choice of Cd(II) and Cu(II) ions is based on their various coordination numbers and geometries. Cd(II) is a group 12 ion, exhibiting a d^{10} electronic configuration without ligand field stabilization. It usually takes distorted tetrahedral, trigonal bipyramidal, and octahedral geometries in complexes [10]. Cu(II) is a typical Jahn–Teller ion with a d^9 electronic subshell and shows coordination geometries from planar square, distorted tetrahedral, square pyramidal, trigonal bipyramidal, to distorted octahedral [11].

In this study, eight compounds, i.e. $(L^1)_2[CdCl_4]$ (**1**), $(L^2)[CdCl_3]$ (**2**), $(L^3)[CdCl_3]$ (**3**), $(L^4)[CdCl_3]$ (**4**), $(L^1)_4[CuCl_4]_2$ (**5**), $(L^2)[CuCl_3]$ (**6**), $(L^3)_2[CuCl_4]$ (**7**), and $(L^4)_2[CuCl_4]$ (**8**), have been prepared and most structurally analyzed (figures 1 and 2). With decrease in the number of hydrogens on nitrogen from three (L^1) to zero (L^4), the anionic structures of the corresponding compounds change from layers (2-D) to chains (1-D) or mononuclear structures. Crystal structures of **1**, **4**, **5**, and **8** have been reported previously [12–22]. However, because of lack of atom coordinates of **1** or inconsistency of reported structures of **5** and **8**, we re-determine and analyze the crystal structures of the three compounds. Unfortunately, the crystal structure of **5** is poorly solved because of low-quality single crystals. So, it is not discussed in detail here.

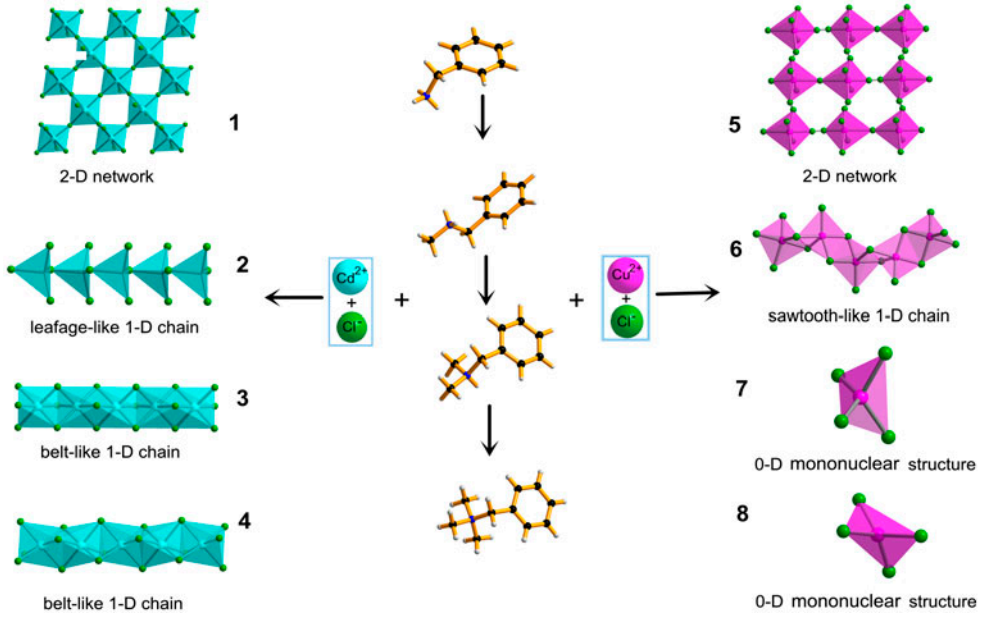

Figure 1. Anionic structures of **1**–**8** in the presence of organic cations.

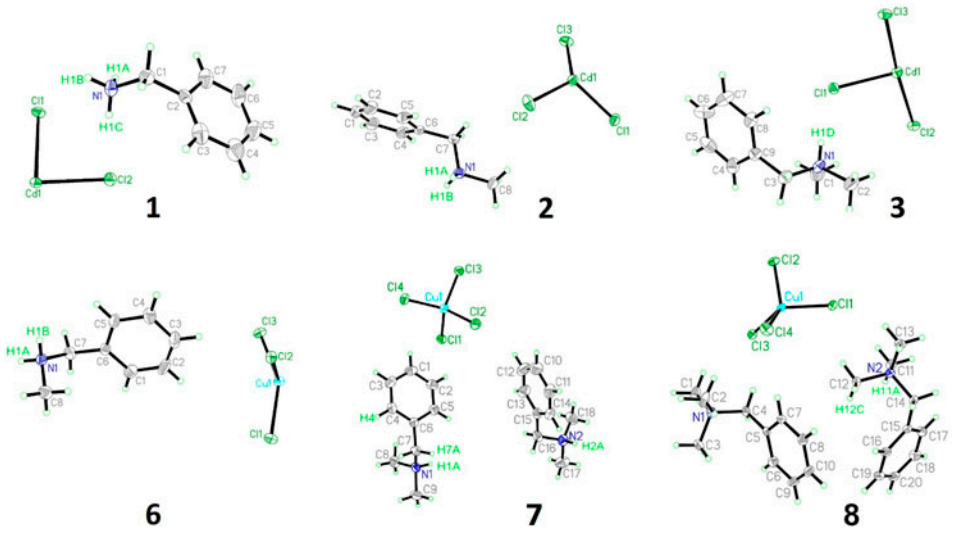

Figure 2. Asymmetric units of **1**–**3** and **6**–**8** showing thermal ellipsoids at the 30% probability level.

2. Experimental

2.1. *Materials and methods*

Analytical grade chemicals were used as received from Aladdin Chemical Ltd, without purification. Infrared (IR) spectra were recorded on a Shimadzu IRPrestige-21 spectrometer. Elemental analyses were measured on a Vario MICRO analyzer (Figure S1, see online supplemental material at http://dx.doi.org/10.1080/00958972.2014.909589). Dielectric measurements were performed on a TongHui 2828 impedance analyzer over the frequency range 200 Hz–1 MHz and the temperature range from 140 to 410 K with an applied electric field of 1.0 V.

Single-crystal data of **1**–**3** and **6** and **7** were collected at 293(2) K on a Rigaku SCXmini CCD diffractometer equipped with graphite-monochromated Mo-Kα radiation ($\lambda = 0.71073$ Å), while the structure of **8** was measured on a Rigaku Saturn 924 diffractometer at 193(2) K. Data processing was performed using the CrystalClear software package (Rigaku, 2005). The structures were solved by direct methods and successive Fourier synthesis and then refined by full-matrix least-squares refinements on F^2 using the SHELXLTL software package (Sheldrick, 2008). Hydrogens bonded to carbon were placed in calculated positions and refined as riding, with C–H = 0.93 Å (benzene ring), C–H = 0.97 Å (methylene), and C–H = 0.96 Å (methyl) with $U_{iso}(H) = 1.2\ U_{eq}(C)$. N-bound H was placed in calculated position with N–H = 0.88−0.91 Å and refined with $U_{iso}(H) = 1.2\ U_{eq}(N)$. Summary of crystallographic data, selected bond lengths and angles, details of hydrogen bonding interactions, and details of weak interactions for the compounds are given in tables 1–4, respectively.

2.2. *Synthesis of 1–3 and 6–8*

2.2.1. Synthesis of $(L^1)_2[CdCl_4]$ (1). Benzylamine hydrochloride (1.436 g, 10 mM) and $CdCl_2{\cdot}2.5H_2O$ (2.284 g, 10 mM) were mixed in distilled water (15 mL). Colorless crystals

were obtained via slow evaporation from the solution at room temperature over 10 days. Yield: 1.927 g (81% based on benzylamine hydrochloride). Anal. Calcd for $C_{14}H_{20}CdCl_4N_2$: C, 35.74; H, 4.28; N, 5.95%. Found: C, 35.67; H, 4.22; N, 5.81%. IR (cm^{-1}, KBr): 3378s, 3219s, 3123s, 3012s, 2997w, 2910w, 1624s, 1570s, 1481s, 1384m, 1211m, 1083s, 1049m, 950w, 866w, 777w, 748s, 692s, 567m.

2.2.2. Synthesis of $(L^2)[CdCl_3]$ (2). *N*-benzylmethylamine hydrochloride (1.575 g, 10 mM) and $CdCl_2{\cdot}2.5H_2O$ (2.284 g, 10 mM) were mixed in water (20 mL). A clear solution was obtained after addition of DMF (3 mL). Colorless crystals were obtained via slow evaporation from the solution at room temperature over 10 days. Yield: 2.53 g (74% based on $CdCl_2{\cdot}2.5H_2O$). Anal. Calcd for $C_8H_{12}CdCl_3N$: C, 28.18; H, 3.55; N, 4.11%. Found: C, 28.13; H, 3.46; N, 4.00%. IR (cm^{-1}, KBr): 3435m, 3138s, 3078s, 2366m, 2341m, 1560s, 1494m, 1456s, 1406s, 1217m, 1149m, 999s, 947m, 894m, 798s, 748s, 692s, 594m.

2.2.3. Synthesis of $(L^3)[CdCl_3]$ (3). *N*,*N*-benzyldimethylamine (10 mM, 1.352 g) was dissolved in 15 mL distilled water after addition of hydrochloric acid solution (37%, 4 mL). Thereafter, $CdCl_2{\cdot}2.5H_2O$ (2.284 g, 10 mM) was added and the precipitate was filtered and dissolved in acetonitrile (20 mL). Colorless crystals were obtained via slow evaporation at room temperature over three days. Yield: 2.307 g (65% based on $CdCl_2{\cdot}2.5H_2O$). Anal. Calcd for $C_9H_{14}CdCl_3N$: C, 30.45; H, 3.98; N, 3.95%. Found: C, 30.34; H, 3.75; N, 3.86%. IR (cm^{-1}, KBr): 3028s, 3001s, 2756s, 1631s, 1469s, 1402m, 1209w, 1157w, 1124w, 1006m, 929s, 829w, 740s, 700s, 592w.

2.2.4. Synthesis of $(L^2)[CuCl_3]$ (6). *N*-benzylmethylamine hydrochloride (1.575 g, 10 mM) and $CdCl_2{\cdot}2H_2O$ (1.705 g, 10 mM) were mixed in water (20 mL), followed by addition of concentrated hydrochloric acid (37%, 1 mL). Orange red crystals were obtained via slow evaporation from the aqueous solution at room temperature over two weeks. Yield: 2.103 g (72% based on $CdCl_2{\cdot}2.5H_2O$). Anal. Calcd for $C_8H_{12}CuCl_3N$: C, 32.90; H, 4.14; N, 4.80%. Found: C, 32.82; H, 4.02; N, 4.72%. IR (cm^{-1}, KBr): 3452m, 3111s, 3055s, 2954m, 2360w, 2333w, 1616w, 1570s, 1498m, 1452s, 1406m, 1379m, 1209w, 1112w, 1022m, 943m, 866s, 740s, 692s, 578m.

2.2.5. Synthesis of $(L^3)_2[CuCl_4]$ (7). *N*,*N*-benzyldimethylamine (1.352 g, 10 mM) and $CdCl_2{\cdot}2H_2O$ (1.705 g, 10 mM) were mixed in ethanol (18 mL), followed by addition of concentrated hydrochloric acid (37%, 10 mL). Orange crystals were obtained via slow evaporation from the aqueous solution at room temperature over two weeks. Yield: 2.107 g (89% based on *N*,*N*-benzyldimethylamine). Anal. Calcd for $C_{18}H_{28}CuCl_4N_2$: C, 45.25; H, 5.91; N, 5.86%. Found: C, 44.97; H, 5.92; N, 5.88%. IR (cm^{-1}, KBr): 3442s, 3076m, 2987s, 2740s, 2333w, 1624s, 1452s, 1402s, 1328w, 1267w, 1211w, 1163m, 1001m, 929s, 829m, 750s, 700s, 596m.

2.2.6. Synthesis of $(L^4)_2[CuCl_4]$ (8). *N*,*N*,*N*-benzyltrimethylamine hydrochloride (10 mM, 1.357 g) and $CdCl_2{\cdot}2H_2O$ (10 mM, 1.705 g) were mixed in water (14 mL). Orange crystals were obtained via slow evaporation at room temperature over 10 days. Yield: 2.025 g (81% based on *N*,*N*,*N*-benzyltrimethylamine hydrochloride). Anal. Calcd for $C_{20}H_{32}CuCl_4N_2$: C,

47.49; H, 6.38; N, 5.54%. Found: C, 47.31; H, 6.31; N, 5.43%. IR (cm^{-1}, KBr): 3427s, 3014m, 2378w, 2326w, 1625s, 1481s, 1450s, 1408m, 1379m, 1217m, 1153w, 1076w, 977m, 918m, 887s, 779s, 727s, 700s, 615w.

3. Results and discussion

3.1. *Synthesis*

Formation of halometallate-based organic–inorganic hybrids would be affected by stoichiometry of metal halides and organic cations, temperature, acidity of the solution, and other external factors. In the case of **1**–**8**, however, their formation was less affected by the reaction stoichiometry and solution acidity, displaying a noticeable structural stability under the reaction conditions. For example, the resulting compounds **1**, **5**, **7**, and **8** have a metal/amine molar ratio of 1 : 2 though the starting materials (metal salts and amines) have a molar ratio of 1 : 1 in the solutions. Therefore, the major factor to determine the formation of **1**–**8** is the type of amine, i.e. the number of N-bonded hydrogens while the reaction stoichiometry exerts less, if any, influence to the anion structures in the corresponding compounds. Compared with the Cu(II) complexes, Cd(II) complexes show relatively low solubilities in aqueous solutions.

3.2. *Crystal structures*

3.2.1. Cd(II) complexes. The crystal structure of **1** was measured by Daoud *et al.* [12, 13], showing a Cmca space group with cell parameters of $a = 7.39$ Å, $b = 32.52$ Å, and $c = 7.59$ Å. However, no further information, such as atom coordinates, is available. Our result discloses that **1** crystallizes in the orthorhombic *Aba2* space group (table 1). It has a 2-D perovskite-type structure [figure 3(a)], which is widely found in a series of organic–inorganic hybrids with a composition formula of $A_2B_{n-1}M_nX_{3n+1}$ ($n = 1$: monolayer, $n > 1$: multilayer), where A and B are organic cations (e.g. alkylamine cations), M is a divalent metal ion, and X is a halide [23]. This type of compounds is potentially useful for magnetic, electrical, and optical properties.

In the anionic layer of **1**, Cd is coordinated by four bridging and two terminal chlorides, resulting in a slightly distorted octahedral geometry [figure 3(b)]. It shows a typical axial compression with the average bond lengths of 2.684 and 2.548 Å for $Cd1-Cl1_{bridging}$ and $Cd1-Cl2_{axial}$, respectively. Adjacent Cd centers are linked by a bridging chloride, giving staggered layers of corner-shared 2-D inorganic perovskite frameworks in the *ac* plane. In the projection parallel to the layers, along the *c* axis, the $CdCl_6$ octahedra are corrugated by an angle of 12.22°, causing a puckering of the layers.

There are two layers of cations embedded between the anionic layers with a head-to-head orientation, spanning nearly half the length of the *c* axis. The amine heads of the cations orient towards the cavities formed by the $CdCl_6$ octahedra through N–H···Cl hydrogen bonding interactions. The hydrogen bonds occur with two terminal halides and three bridging halides [figure 3(c) and table 3], forming a terminal halide configuration [24]. The cations in the same layer have two orientations with a dihedral angle of 67.49° between the aromatic planes. There are weak interactions among the phenyl rings with an edge-to-face

Table 1. Crystallographic data and structural refinement details for **1**–**3** and **6**–**8**.

	1	**2**	**3**	**6**	**7**	**8**
Formula	$C_{14}H_{20}CdCl_4N_2$	$C_8H_{12}CdCl_3N$	$C_9H_{14}CdCl_3N$	$C_8H_{12}CuCl_3N$	$C_{18}H_{28}Cl_4CuN_2$	$C_{20}H_{32}Cl_4CuN_2$
Formula weight	470.52	340.94	354.96	292.08	477.76	505.82
T (K)	293(2)	293(2)	293(2)	293(2)	293(2)	193(2)
Crystal size (mm)	0.3 × 0.3 × 0.2	0.3 × 0.3 × 0.2	0.3 × 0.2 × 0.2	0.3 × 0.2 × 0.2	0.3 × 0.3 × 0.3	0.3 × 0.3 × 0.2
Crystal system	Orthorhombic	Monoclinic	Monoclinic	Monoclinic	Triclinic	Monoclinic
Space group	*Aba2*[d]	*P2₁/c*	*Cc*	*C2/c*	*P−1*	*P2₁/c*
a (Å)	7.5888(15)	8.1014(16)	13.776(3)	23.419(5)	7.9793(16)	9.535(3)
b (Å)	32.738(6)	24.796(5)	14.945(3)	8.2341(16)	12.255(3)	9.059(3)
c (Å)	7.5041(15)	6.0575(12)	6.7520(14)	12.003(2)	13.007(3)	29.373(9)
α (°)	90	90	90	90	72.18(3)	90
β (°)	90	92.81(3)	112.57(3)	100.96(3)	76.13(3)	106.578(10)
γ (°)	90	90	90	90	73.99(3)	90
V (Å^3)	1864.3(6)	1215.4(4)	1283.6(5)	2272.4(8)	1147.0(4)	2432(1)
Z	4	4	4	8	2	4
D_{Calcd} (g cm^{-3})	1.676	1.863	1.837	1.707	1.383	1.382
μ (mm^{-1})	1.739	2.413	2.289	2.582	1.422	1.346
F (0 0 0)	936	664	696	1176	494	1052
θ Range (°)	3.66−27.45	3.01−27.44	3.20−27.47	3.05−27.46	3.34−27.46	2.28−27.48
Reflns. collected	8422	12,612	6584	11,415	12,039	25,883
Independent reflns. (R_{int})	2125(0.0596)	2771 (0.0634)	2909 (0.0220)	2599 (0.0355)	5254 (0.0410)	5535 (0.0515)
No. parameters	98	119	128	120	231	250
R_1[a], wR_2[b] [$I > 2\sigma(I)$]	0.0339, 0.0503	0.0418, 0.0674	0.0170, 0.0397	0.0226, 0.0557	0.0458, 0.0868	0.0521, 0.1227
R_1, wR_2 [all data]	0.0406, 0.0524	0.0639, 0.0732	0.0177, 0.0399	0.0249, 0.0567	0.0688, 0.0964	0.0659, 0.1291
GOF	0.967	1.085	1.11	1.088	1.081	1.152
$\Delta\rho$[c] (e Å^{-3})	0.744, −0.508	0.501, −0.471	0.197, −0.379	0.438, −0.329	0.358, −0.308	0.349, −0.440

[a] $R_1 = \Sigma||F_o| - |F_c||/\Sigma|F_o|$.
[b] $wR_2 = [\Sigma w(F_o^2 - F_c^2)^2/\Sigma w(F_o^2)^2]^{1/2}$.
[c] Maximum and minimum residual electron density.
[d] The space group *Aba2* (41) is now indicated as *Aea2* (41). See: Ref. [50].

Table 2. Selected bond distances (Å), angles, and torsion angles (°) around metal ions in **1**–**3** and **6**–**8**.

Atoms	Angle (°)	Atoms	Distance (Å)
1			
Cl(2)−Cd(1)−Cl(2)^{i}	169.63(5)	Cd(1)−Cl(1)	2.725(2)
Cl(2)−Cd(1)−Cl(1)^{ii}	93.18(3)	Cd(1)−Cl(2)	2.5475(9)
Cl(2)−Cd(1)−Cl(1)^{iii}	94.29(3)	Cd(1)−Cl(1)^{ii}	2.642(2)
Cl(1)^{ii}−Cd(1)−Cl(1)^{iii}	87.74(9)		
Cl(2)−Cd(1)−Cl(1)	86.53(3)		
Cl(2)^{i}−Cd(1)−Cl(1)	86.45(3)		
Cl(1)^{ii}−Cd(1)−Cl(1)	176.52(9)		
Cl(1)−Cd(1)−Cl(1)^{i}	94.62(9)		
Cd(1)^{iv}−Cl(1)−Cd(1)	167.79(3)		
Cl(2)−Cd(1)−Cl(1)−Cd(1)^{iv}	−18.1(4)		
Cl(1)^{ii}−Cd(1)−Cl(1)−Cd(1)^{iv}	−103.5(5)		
Cl(1)^{i}−Cd(1)−Cl(1)−Cd(1)^{iv}	68.0(4)		
Symmetry transformations	(i) $-x+2, -y+2, z$; (ii) $x+1/2, -y+2, z+1/2$; (iii) $-x+3/2, y, z+1/2$; (iv) $-x+3/2, y, z-1/2$		
2			
Cl(2)−Cd(1)−Cl(3)	125.28(5)	Cd(1)−Cl(2)	2.379(1)
Cl(2)−Cd(1)−Cl(1)	113.16(5)	Cd(1)−Cl(3)	2.428(1)
Cl(3)−Cd(1)−Cl(1)	112.92(4)	Cd(1)−Cl(1)	2.513(1)
Cl(2)−Cd(1)−Cl(1)^{i}	107.37(5)	Cd(1)−Cl(1)^{i}	2.619(1)
Cl(3)−Cd(1)−Cl(1)^{i}	97.39(5)		
Cl(1)−Cd(1)−Cl(1)^{i}	93.77(3)		
Cd(1)−Cl(1)−Cd(1)^{ii}	105.12(4)		
Cl(2)−Cd(1)−Cl(1)−Cd(1)^{ii}	68.11(6)		
Cl(3)−Cd(1)−Cl(1)−Cd(1)^{ii}	−81.54(6)		
Cl(1)^{i}−Cd(1)−Cl(1)−Cd(1)^{ii}	178.808(9)		
Symmetry transformations	(i) $x, -y+1/2, z+1/2$; (ii) $x, -y+1/2, z-1/2$		
3			
Cl(2)−Cd(1)−Cl(1)	100.33(3)	Cd(1)−Cl(3)^{i}	2.593(1)
Cl(1)−Cd(1)−Cl(2)^{i}i	83.42(3)	Cd(1)−Cl(3)	2.6080(9)
Cl(3)^{i}−Cd(1)−Cl(1)^{i}	82.68(3)	Cd(1)−Cl(2)	2.637(1)
Cl(3)^{i}−Cd(1)−Cl(3)	98.86(4)	Cd(1)−Cl(1)	2.6612(8)
Cl(2)−Cd(1)−Cl(1)^{i}	82.66(3)	Cd(1)−Cl(2)^{ii}	2.663(1)
Cl(1)−Cd(1)−Cl(1)^{i}	176.52(4)	Cd(1)−Cl(1)^{i}	2.7257(9)
Cl(2)^{ii}−Cd(1)−Cl(1)^{i}	98.33(3)	Cd(1)−Cd(1)^{i}	3.3768(7)
Cd(1)^{ii}−Cd(1)−Cd(1)^{i}	177.44(1)		
Cl(3)^{i}−Cd(1)−Cl(1)−Cd(1)^{ii}	−140.14(2)		
Cl(2)−Cd(1)−Cl(1)−Cd(1)^{ii}	133.76(3)		
Cl(2)^{ii}−Cd(1)−Cl(1)−Cd(1)^{ii}	43.19(3)		
Cd(1)^{i}−Cd(1)−Cl(1)−Cd(1)^{ii}	−179.873(2)		
Cl(1)−Cd(1)−Cl(2)−Cd(1)^{i}	134.73(2)		
Cl(1)^{i}−Cd(1)−Cl(2)−Cd(1)^{i}	−43.46(2)		
Symmetry transformations	(i) $x, -y+1, z-1/2$; (ii) $x, -y+1, z+1/2$		
6			
Cl(2)−Cu(1)−Cl(1)	92.12(2)	Cl(1)−Cu(1)	2.2751(6)
Cl(2)−Cu(1)−Cl(3)^{ii}	176.84(2)	Cl(2)−Cu(1)	2.2736(8)
Cl(2)−Cu(1) −Cl(3)	93.11(2)	Cu(1)−Cl(2)^{i}	2.6651(8)
Cl(1)−Cu(1)−Cl(3)	152.14(2)	Cl(3)−Cu(1)^{ii}	2.3157(8)
Cl(3)^{ii}−Cu(1)−Cl(3)	85.27(2)	Cl(3)−Cu(1)	2.3180(6)
Cl(2)−Cu(1)−Cl(2)^{i}	86.63(3)		
Cl(1)−Cu(1)−Cl(2)^{i}	109.77(2)		
Cl(3)−Cu(1)−Cl(2)^{i}	97.85(2)		
Cu(1)^{i}−Cl(2)−Cu(1)−Cl(1)	95.00(2)		

(*Continued*)

Table 2. (*Continued*).

Atoms	Angle (°)	Atoms	Distance (Å)
$Cu(1)^{i}$–Cl(2)–Cu(1)–$Cl(3)^{ii}$	−53.5(3)		
$Cu(1)^{i}$–Cl(2)–Cu(1)–$Cl(2)^{i}$	−14.68(2)		
$Cu(1)^{ii}$–Cl(3)–Cu(1)–Cl(2)	177.29(2)		
$Cu(1)^{ii}$–Cl(3)–Cu(1)–$Cl(2)^{i}$	90.26(3)		
Symmetry transformations	(i) $-x, y, -z+1/2$; (ii) $-x, -y+1, -z$		
7			
Cl(4)–Cu(1)–Cl(2)	134.52(4)	Cl(1)–Cu(1)	2.263(1)
Cl(4)–Cu(1)–Cl(1)	102.41(5)	Cl(2)–Cu(1)	2.237(1)
Cl(2)–Cu(1)–Cl(1)	97.91(5)	Cl(3)–Cu(1)	2.300(1)
Cl(4)–Cu(1)–Cl(3)	100.64(4)	Cl(4)–Cu(1)	2.219(1)
Cl(2)–Cu(1)–Cl(3)	101.64(4)		
Cl(1)–Cu(1)–Cl(3)	122.84(4)		
8			
Cl(4)–Cu(1)–Cl(1)	100.03(5)	Cl(1)–Cu(1)	2.258(1)
Cl(4)–Cu(1)–Cl(2)	131.59(4)	Cl(2)–Cu(1)	2.262(1)
Cl(1)–Cu(1)–Cl(2)	98.87(4)	Cl(3)–Cu(1)	2.269(1)
Cl(4)–Cu(1)–Cl(3)	99.22(4)	Cl(4)–Cu(1)	2.228(1)
Cl(1)–Cu(1)–Cl(3)	133.13(4)		
Cl(2)–Cu(1)–Cl(3)	99.42(4)		

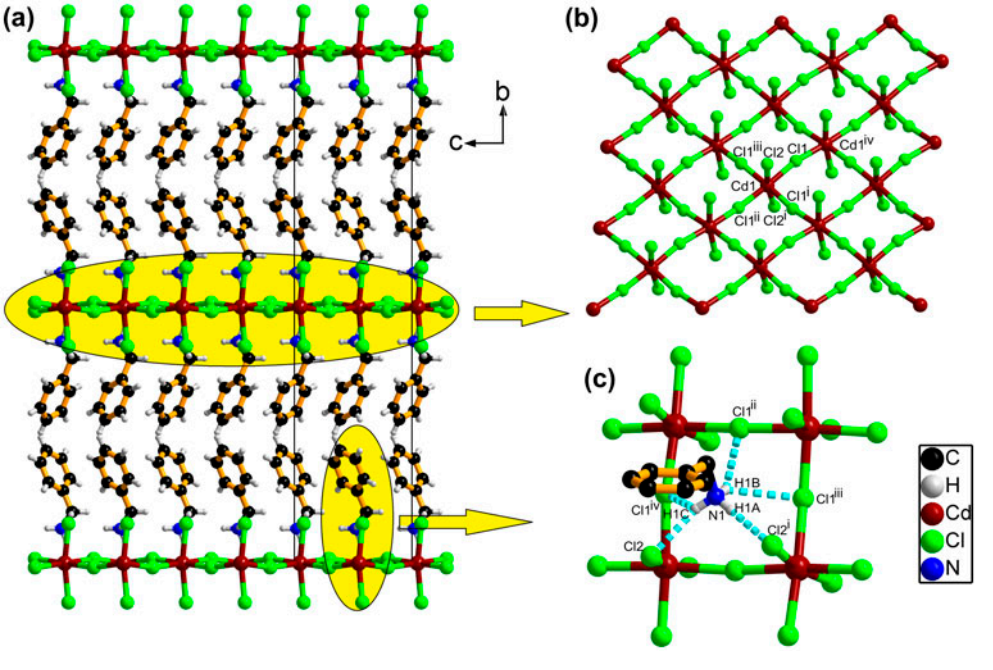

Figure 3. (a) Packing diagram of **1** viewed along the *a* axis. (b) Layer structure of the anionic part in **1**. (c) Hydrogen bonding interactions between the benzylamine cation and the inorganic layer in **1**.

Table 3. Hydrogen bonds in **1**–**3**, **6**, and **7**.

D−H···A	D···A (Å)	Symmetry transformations
1		
N(1)−H(1A)···Cl(2)^{i}	3.205(3)	(i) $-x+3/2$, y, $z-1/2$
N(1)−H(1B)···Cl(1)^{ii}	3.530(4)	(ii) $x+1/2$, $-y+2$, $z-1/2$
N(1)−H(1B)···Cl(1)^{iii}	3.568(3)	(iii) $x+3/2$, $3/2-y$, z
N(1)−H(1C)···Cl(1)^{iv}	3.421(4)	(iv) $-x+2$, $-y+2$, z
N(1)−H(1C)···Cl(2)	3.306(4)	
2		
N(1)−H(1A)···Cl(3)^{i}	3.313(4)	(i) $x+1$, y, z
N(1)−H(1B)···Cl(3)^{ii}	3.330(4)	(ii) $x+1$, y, $z-1$
3		
N(1)−H(1D)···Cl(1)	3.154(2)	
6		
N(1)−H(1A)···Cl(1)^{i}	3.318(2)	(i) $x+1/2$, $y-1/2$, z
N(1)−H(1A)···Cl(1)^{iii}	3.386(2)	(ii) $-x+1/2$, $y-1/2$, $-z+1/2$
N(1)−H(1B)···Cl(1)^{ii}	3.261(2)	(iii) $-x+1/2$, $-y+3/2$, $-z$
N(1)−H(1B)···Cl(2)^{ii}	3.492(2)	
7		
N(1)−H(1A)···Cl(1)^{i}	3.279(3)	(i) $-x$, $-y+1$, $-z+1$
N(1)−H(1A)···Cl(2)^{i}	3.436(3)	(ii) x, y, $z+1$
N(2)−H(2A)···Cl(3)^{ii}	3.166(3)	

(EF) motif, which occurs between the hydrogen from one phenyl ring and the centroid of the adjacent ring [25].

In **2**–**4**, three *N*-methylated derivatives of benzylamine, i.e. *N*-benzylmethylamine, *N*,*N*-benzyldimethylamine, and *N*,*N*,*N*-benzyltrimethylamine, are employed as cations. The structures of the three compounds are anionic chains, different from **1**.

Cd(II) in **2** is tetrahedrally coordinated by two bridging and two terminal chlorides (figure 4). The Cd−Cl bond lengths and Cl−Cd−Cl bond angles range from 2.379(1) to 2.619(1) Å and 93.77(3)°–125.28(4)°, respectively, indicating a moderately distorted tetrahedral geometry. As a basic building unit, the [$CdCl_4$] monomers are interconnected by two bridging chlorides to form a corner-shared zigzag chain, a rare type of chain in Cd(II)-containing complexes. A weak interaction exists between the Cd ion and neighboring bridging Cl^- with a distance of 3.478 Å, which may contribute to the stability of the chain.

Structures of the anionic chains in **3** and **4** are the same, but different from the one in **2** (figure 1). In the two compounds, Cd is coordinated by six bridging chlorides with Cd−Cl bond lengths of 2.608(1)−2.668(2) Å and Cd−Cl−Cd bond angles of 77.63(2)°−80.96(3)°. Adjacent Cd centers have a distance of 3.38 Å and are connected through three bridging chlorides to give a chain in which the metal octahedra are all face shared. This type of chain structure is found in some chlorocadmate(II) complexes [26, 27].

The inorganic anionic chains in **2**–**4** arrange alternately around which lie the organic cations. In **2**, each $-NH_2(CH_3)$ head of the cation is hydrogen bonded with two adjacent terminal chlorides of the chain (N(1)−H(1A)···Cl(3)^{i} and N(1)−H(1B)···Cl(3)^{ii}). For **3**, each organic cation participates in one hydrogen bond between $-NH(CH_3)_2$ and one bridging chloride with a N···Cl distance of 3.154 Å (figure 5). There are no N–H···Cl hydrogen bonds in **4** due to the lack of active hydrogens of the organic cations. However, weak

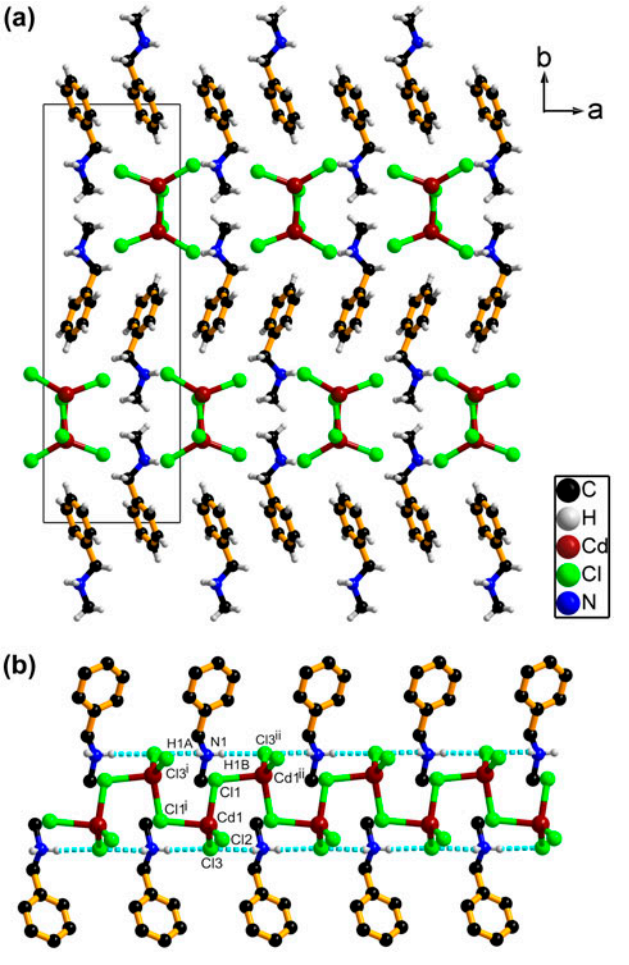

Figure 4. (a) Packing diagram of **2** viewed along the *c* axis and (b) hydrogen bonds in the chain in **2**.

C–H•••Cl interactions are still widespread among the chlorides and the hydrogens of the alkyl and phenyl groups [19].

3.2.2. Cu(II) complexes. Compound **5** was studied by several research groups for its magnetic and catalytic properties [14–18]. Its structure was considered to be the well-known 2-D perovskite-type structure, similar to **1**. Numerous similar compounds have been explored by varying the organic cations [28–35]. Reported crystal data of a compound with the same components of **5** indicate that it adopts a triclinic *P1* space group with cell parameters of $a = 10.444(2)$ Å, $b = 10.492(2)$ Å, $c = 15.979(3)$ Å, $\alpha = 98.43(3)°$, $\beta = 99.49(3)°$, and $\gamma = 90.00(3)°$ [18]. In our study, **5** is found to crystallize in a different triclinic *P−1* space group but with very similar cell parameters of $a = 10.501(2)$ Å, $b = 10.576(2)$ Å, $c = 16.115(3)$ Å, $\alpha = 98.00(3)°$, $\beta = 99.33(3)°$, and $\gamma = 90.06(3)°$. Unfortunately, structure solution failed because of the low quality of the single crystals of **5**. Further study is needed to afford more accurate structural data of the compound by obtaining high-quality single crystals.

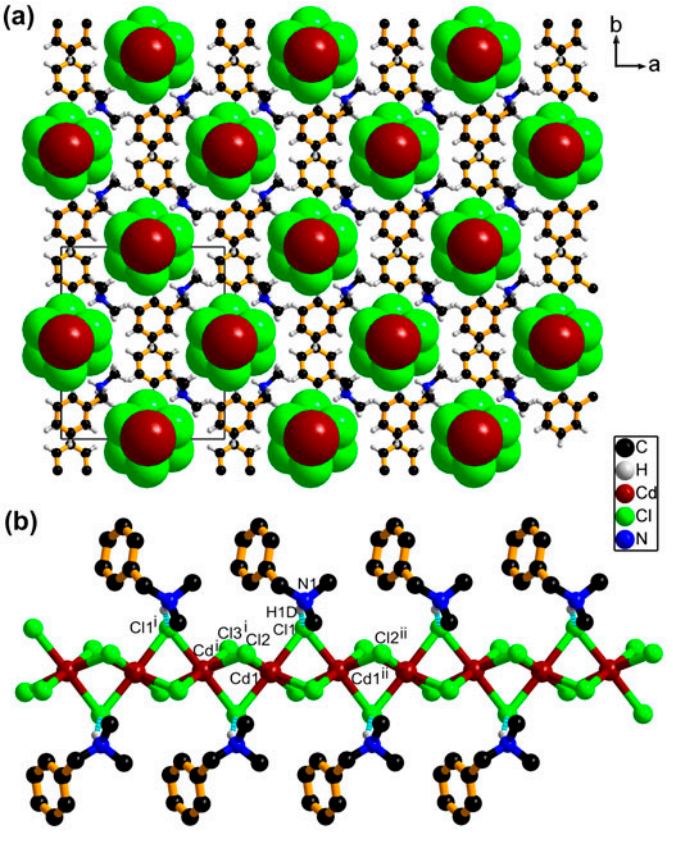

Figure 5. (a) Packing diagram of **3** viewed along the *c* axis and (b) hydrogen bonds in the chain in **3**.

Compound **6** consists of *N*-benzylmethylamine cations and anionic $[CuCl_3]$ chains (figure 2). This type of chain structure was found in several compounds [36–39]. Repeated unit of the chain is $[Cu_4Cl_{12}]^{4-}$ tetramers (figure 6). The four Cu−Cl distances are 2.2736 (8)−2.3180(6) Å. Neighboring tetramers are linked to each other through a bridging $Cl2^{iii}$ with a much longer bond (2.6651(8) Å), indicating a weak interaction. So, Cu1 is coordinated by four bridging chlorides (Cl2, $Cl2^{iii}$, Cl3, and $Cl3^{ii}$) and one terminal (Cl1), showing a distorted trigonal bipyramidal geometry. The bond angle of Cl2−Cu1−$Cl3^{ii}$ is 176.84 (2)°, almost perpendicular to the plane formed by Cl1, $Cl2^{iii}$, and Cl3. Every two adjacent Cu(II) ions share two bridging chlorides as a common edge. The Cu1−$Cu1^{ii}$ distance is 3.4091(7) Å. The resulting chain extends along the *c* axis. There are four hydrogen bonds between $-NH_2(CH_3)$ head of the cations and the inorganic chains, resulting in formation of supramolecular layers in the *bc* plane.

In **7** and **8**, the anions are all isolated $[CuCl_4]^{2-}$ ions. Cu(II) adopts a distorted tetrahedral geometry with approximate D_{2d} symmetry. The Cu−Cl bond distances are 2.219(1)−2.300 (1) Å for **7** and 2.228(1)−2.269(1) Å for **8**, falling within the normal range of $[CuCl_4]^{2-}$ (2.223−2.284 Å) [40–43]. The Cl−Cu−Cl bond angles of 97.91(5)°−134.52(4)° for **7** and 98.87(4)°−133.13(4)° for **8** are in the range of reported values (142.64°−96.78°), reflecting

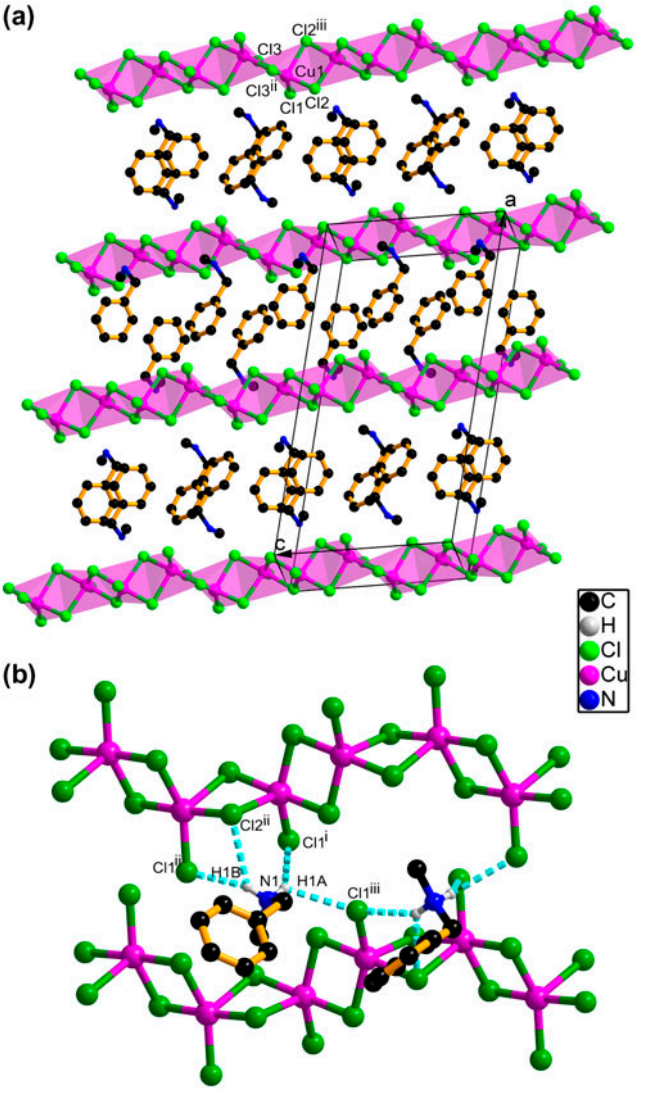

Figure 6. (a) Packing diagram of **6** and (b) hydrogen bonding interactions between the cation and inorganic chain in **6**.

an intermediate coordination structure of Cu(II) between distorted tetrahedral and square-planar geometries. The cations in **7** form N–H···Cl hydrogen bonds with the $[CuCl_4]^{2-}$ and aromatic rings of the cations show C–H···π interactions (2.8837 Å) with an EF motif (figure 7). For **8**, there are no classical hydrogen bonds between the *N*,*N*,*N*-benzyltrimethylamine cation and $[CuCl_4]^{2-}$ [20–22]. However, C–H···Cl interactions exist to arrange the organic cations and inorganic anions, together with C–H···π interactions (figure 8 and table 4).

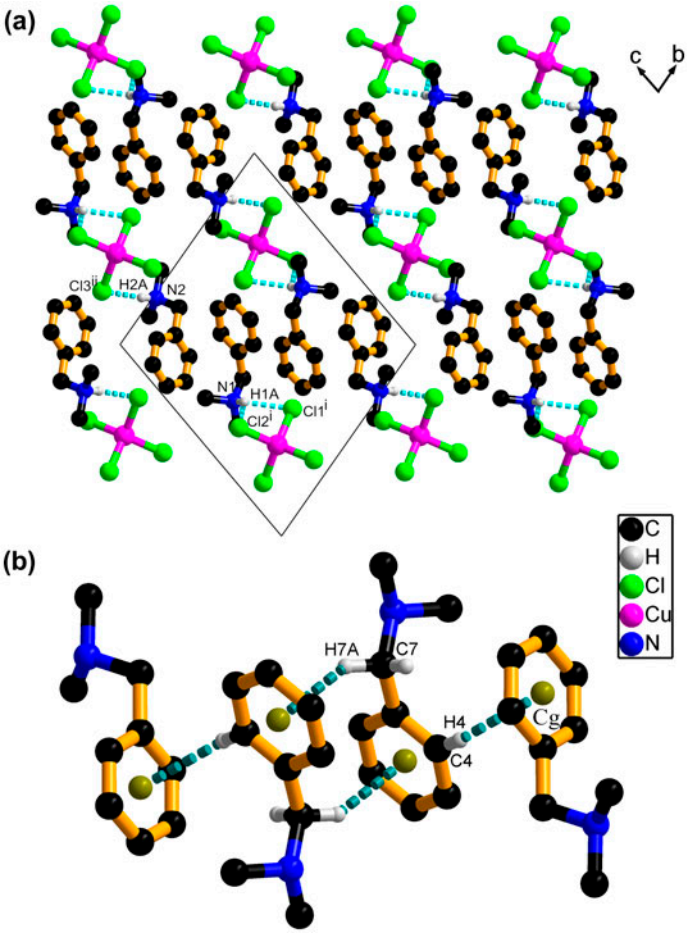

Figure 7. (a) Packing diagram of **7** viewed along the *a* axis and (b) C–H···π interactions in **7**.

3.2.3. Role of the ligands. Organic cations often play a key role in the formation of inorganic anionic networks through their shapes, sizes, and various intermolecular interactions such as hydrogen bonds, van der Waals interactions, and ionic bonds [5–7]. L^1–L^4 show their influence on the anionic structures in **1**–**8**. With the increase in methyl groups on N of the amine, the ligands become larger and more hydrophobic and lose the propensity to develop hydrogen bonds with the anions. As a result, the anionic structures change from layers to chains in **1**–**4** and to mononuclear species in **5**–**8**.

For L^1, the terminal amine has three hydrogens that can form at least three hydrogen bonds with inorganic anions. These interactions stabilize the resulting 2-D perovskite-type structures shown as $[RNH_3]_2[MX_4]$ (R = alkyl group). The cations are generally primary amines which can form five hydrogen bonds as seen in **1**, varying from strong to weak (N···Cl distances of 3.205(3)−3.568(3) Å) (table 3). This should be a key factor to formation of **1** and **5** that have 2-D perovskite-type structures. Compared with L^1, L^2 is *N*-monomethylated and still has two hydrogens to yield hydrogen bonds. Correspondingly,

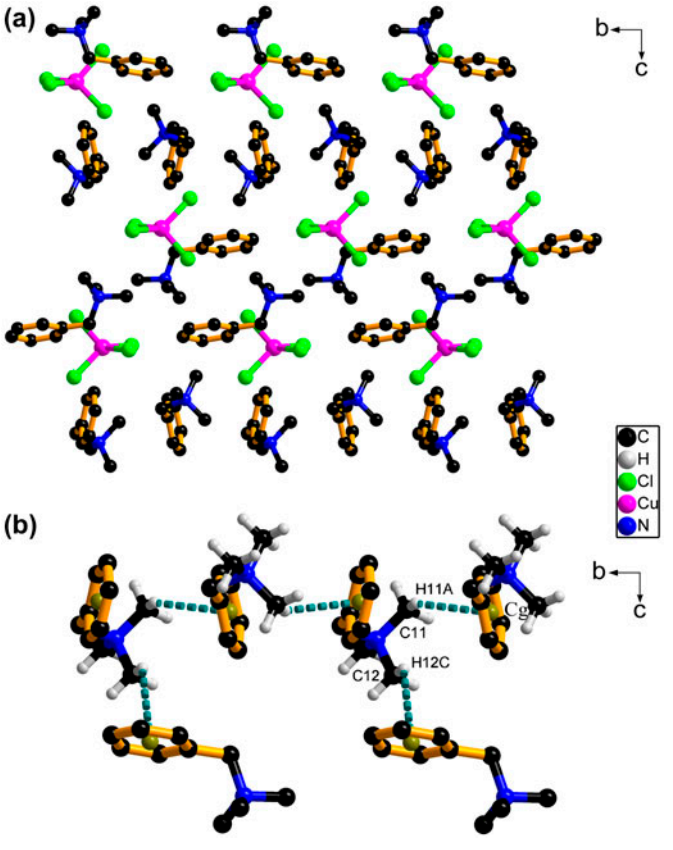

Figure 8. (a) Packing diagram of **8** viewed along the *a* axis and (b) C–H···π interactions in **8**.

Table 4. Weak interactions in **2**, **3**, **7**, and **8**.

D−H···A	D···A (Å)	Symmetry transformations
2		
C(8)−H(8A)···Cl(2)	3.657(4)	(i) $-x+3/2$, y, $z-1/2$
C(8)−H(8C)···Cl(2)^{i}	3.803(5)	
3		
C(1)−H(1C)···Cl(3)	3.624(3)	(i) $x+1/2$, $y+1/2$, z
C(3)^{i}−H(3A)^{i} ···Cl(3)^{ii}	3.593(2)	(ii) $x+1$, y, $z+1$
7		
C(4)−H(4)···Cg[a]	3.784(3)	
C(7)−H(7A)···Cg	3.418(4)	
8		
C(11)−H(11A)···Cg	3.883(4)	
C(12)−H(12C)···Cg	3.998(4)	

[a]Cg denotes the center of phenyl ring.

the number of hydrogen bonds in **2** is less than that in **1** while there are still four hydrogen bonds in **6**. However, this modification makes L^2 different from L^1, which causes **2** and **6** to develop anionic chain structures. Further methylation leads to L^3 and L^4, both of which show similarities in the effect on the structures of the corresponding compounds, i.e. chains in **3** and **4**, and mononuclear species in **7** and **8**.

The structural difference between **2** and **3** is clear and interesting. They have the same metal/amine molar ratio but with different anionic chain structures, i.e. the coordination number of Cd(II) changes from four in **2** to six in **3**. By analyzing the respective fragment of **2**, one can see that each organic cation stabilizes the conformation of neighboring $CdCl_4$ tetrahedra by two N–H···Cl hydrogen bonds from one side and four weak C–H···Cl interactions from the other side, causing all the terminal chlorides in the chain to be bonded by two types of interactions, i.e. either strong N–H···Cl hydrogen bonding interactions or weak C–H···Cl interactions (figure 9 and table 4). Such stabilization is not possible in **3**, where there is only one N–H···Cl hydrogen bond or at most two C–H···Cl interactions to each bridging chloride. As a compensation, attractive electrostatic force between Cl^- and Cd(II) forms additional bonds to complete the coordination number of Cd(II) to six in **3** but not four in **2**.

This dominating Cd−Cl interaction is preserved in **4** without any strong N–H···Cl hydrogen bonds at all. Because of the lack of interactions with the terminal chlorides like in **2**, **4** shows a similar anionic chain structure with **3**. The effect of the organic cations on **3** and **4** is observable, i.e. the compounds show different chain structures, while the effect of the

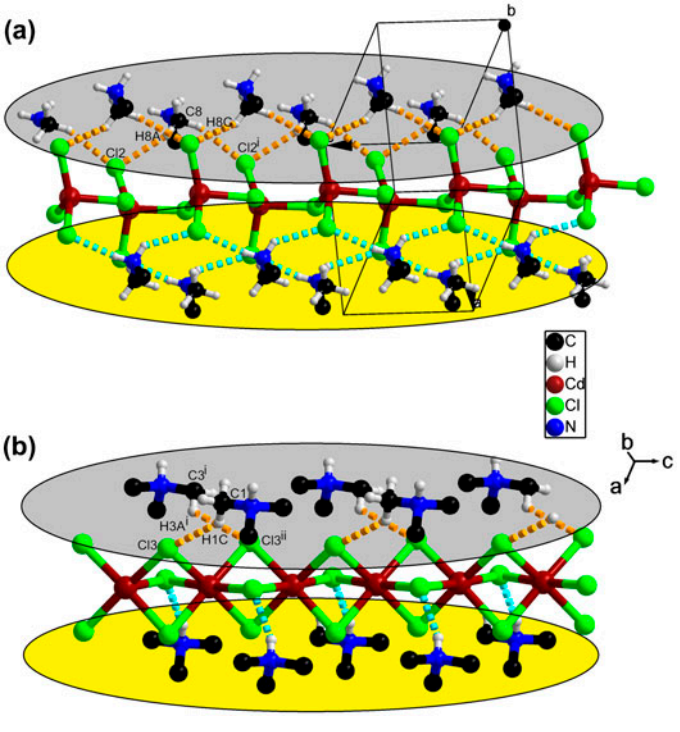

Figure 9. (a) Hydrogen bonding interactions and C–H···Cl interactions between the cation and inorganic chain in **2** and (b) hydrogen bonding interactions and C–H···Cl interactions between the cation and inorganic chain in **3**. Aromatic rings are omitted for clarity.

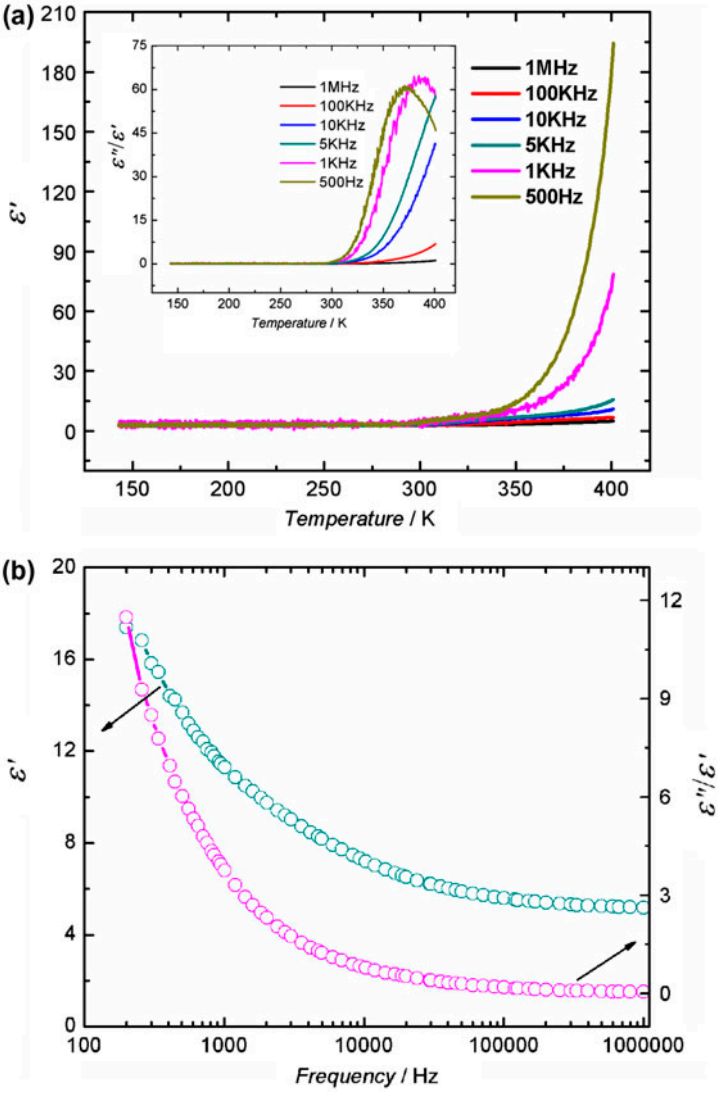

Figure 10. (a) Temperature-dependent dielectric constant of **2** measured at 1 MHz. Inset: the spectra measured at several frequencies and (b) frequency-dependent dielectric constant of **2** measured from 200 Hz−1 MHz at room temperature.

cations on **7** and **8** seems negligible. The difference between the Cd(II) and Cu(II) complexes is based on the metal ions themselves because the Cd(II) centers tend to be more highly coordinated by halides than Cu(II) centers.

When comparing the structural difference of **6** and **7**, one can see that each organic cation stabilizes the conformation of two adjacent 1-D chains by four N–H···Cl hydrogen bonds in **6**. Such stabilization does not occur in **7**, where there are only three hydrogen bonds. Thus, the 1-D chain in **6** breaks down into distorted tetrahedral anionic structures in **7** and **8** with no N–H···Cl hydrogen bonds at all. Weaker C–H···π interactions among the

aromatic groups contributes to the crystal packing in these compounds, particularly obvious in **7** and **8** (table 4).

3.3. *Dielectric constant measurements*

For most molecules, dielectricity is a fundamental property to reflect their polarizabilities under an electric field. It is described by a dielectric constant $\varepsilon (= \varepsilon' - i\varepsilon''$, where ε' is the real part and ε'' the imaginary part). Information about the molecular motions and changes can be disclosed by dielectric constant measurements such as those in dielectric switching and ferroelectric phase transitions [44–47].

As a preliminarily study, the dielectric constants of **1**–**8** were measured from 140 to 410 K, and the frequency range 200 Hz−1 MHz (figures S2 and S3). Taking **2,** for example, temperature-dependent dielectric constant shows that ε′ is constant below 300 K at ca. 2.64 at 1 MHz and increases rapidly above 300 K to reach a maximum of 4.91 at 401 K (figure 10). The ε' adopts a similar trend at other frequencies. The dielectric loss ($\varepsilon''/\varepsilon'$) reveals a similar trend to that of ε'. On the other hand, frequency-dependent dielectric constant shows that the ε' drops sharply with increase in frequency. These changes, i.e. increases in the dielectric constant at higher temperatures and lower frequencies, can be attributed to the space charge polarization [48]. No dielectric anomalies occur in the measured temperature range for **1**–**8**, indicating no dynamic changes in the architectures of these compounds [49].

4. Conclusion

Inorganic–organic hybrid compounds **1**–**8** based on Cd(II) and Cu(II) chlorides have been synthesized by employing protonated benzylamine and its *N*-methylated derivatives, $[C_6H_5CH_2NH_{3-n}(CH_3)_n]^+$ ($n = 0-3$), as cations. The organic cations show influence on the anionic structures via intermolecular interactions, especially hydrogen bonds. With the increase in methyl groups on N of the amine, the anionic structures of the compounds change from perovskite-type layers to chains in Cd(II) compounds (**1**–**4**) and to mononuclear species in Cu(II) compounds (**5**–**8**).

Supplementary material

CCDC 957345−957347, 957470, 903708, 980306 contain the supplementary crystallographic data for **1**–**3** and **6**–**8**, respectively. These data can be obtained free of charge via http://www.ccdc.cam.ac.uk/conts/retrieving.html, or from the Cambridge Crystallographic Data Center, 12 Union Road, Cambridge CB2 1EZ, UK; Fax: +44 1223-336-033; or E-mail: deposit@ccdc.cam.ac.uk. Supplementary data associated with this article can be found, in the online version, at http://dx.doi.org/10.1016/j.poly.

Funding

This work was financially supported by MEC [grant number NCET-10-0333].

References

[1] J.W. Steed. *Supramolecular Chemistry*, Wiley, West Sussex (2000).
[2] G.R. Desiraju. *Crystal Engineering: The Design of Organic Solids*, Elsevier, Amsterdam (1989).
[3] S. Horiuchi, Y. Tokura. *Nat. Mater.*, **7**, 357 (2008).
[4] W. Zhang, R.-G. Xiong. *Chem. Rev.*, **112**, 1163 (2012).
[5] J.L. Atwood, J.E.D. Davies, D.D. MacNicol, F. Voegtle (Eds). *Comprehensive Supramolecular Chemistry*, Vol. 11, Pergamon, Oxford (1996).
[6] D. Braga, F. Grepioni, G. Desiraju. *Chem. Rev.*, **98**, 1375 (1998).
[7] A.M. Beatty. *Coord. Chem. Rev.*, **246**, 131 (2003).
[8] G.A. Jeffrey. *An Introduction to Hydrogen Bonding*, Oxford University Press, Oxford, (1997).
[9] C.B. Aakeröy, K.R. Seddon. *Chem. Soc. Rev.*, **22**, 397 (1993).
[10] C.-L. Chen, A.M. Beatty. *Chem. Commun.*, 76 (2007).
[11] R.D. Willett. *Coord. Chem. Rev.*, **109**, 181 (1991).
[12] A. Daoud, R. Perret. *Bull. Soc. Chim. Fr.*, **3–4**, 657 (1974).
[13] A. Daoud. *Bull. Soc. Chim. Fr.*, **9–10**, 1418 (1976).
[14] A. Daoud, T.S. Aline, P. Rene, C. Bernard, E.G. Jacques. *Bull. Soc. Chim. Fr.*, **3–4**, 535 (1975).
[15] A. Dupas, K. Le Dang, J.P. Renard, P. Veillet, A. Daoud, R. Perret. *J. Chem. Phys.*, **65**, 4099 (1976).
[16] W.E. Estes, D.B. Losee, W.E. Hatfield. *J. Chem. Phys.*, **72**, 630 (1980).
[17] Y. Kimishima. *J. Magn. Magn. Mater.*, **90–91**, 301 (1990).
[18] S. Löw, J. Becker, C. Würtele, A. Miska, C. Kleeberg, U. Behrens, O. Walter, S. Schindler. *Chem. Eur. J.*, **19**, 5342 (2013).
[19] D.-H. Wu, L. Jin. *Acta Cryst.*, **C69**, 491 (2013).
[20] C. Furlani, G. Morpurgo. *Theor. Chim. Acta*, **1**, 102 (1963).
[21] M. Bonamico, G. Dessy, A. Vaciago. *Theor. Chim. Acta*, **7**, 367 (1967).
[22] N. Gálvez, M. Moreno-Mañas, I. Padrós, R.M. Sebastián, N. Serra, A. Vallribera. *Polyhedron*, **14**, 1397 (1995).
[23] D.B. Mitzi. *Synthesis, Structure, and Properties of Organic–Inorganic Perovskites and Related Materials (Progress in Inorganic Chemistry)*, Wiley, San Francisco, CA (1999).
[24] D.B. Mitzi. *J. Chem. Soc., Dalton Trans.*, 1 (2001).
[25] V. Russell, M. Scudder, I. Dance. *J. Chem. Soc., Dalton Trans.*, 789 (2001).
[26] F.F. Jian, P.S. Zhao, Q.X. Wang, Y. Li. *Inorg. Chim. Acta*, **359**, 1473 (2006).
[27] C.E. Costin-Hogan, C.-L. Chen, E. Hughes, A. Pickett, R. Valencia, N.P. Rath, A.M. Beatty. *CrystEngComm*, **10**, 1910 (2008).
[28] J.P. Steadman, R.D. Willett. *Inorg. Chim. Acta*, **4**, 367 (1970).
[29] F. Barendregt, H. Schenk. *Physica*, **49**, 465 (1970).
[30] L.J. De Jongh, A.R. Miedema. *Adv. Phys.*, **23**, 1 (1974).
[31] C.P. Landee, K. Halvorson, R.D. Willett. *J. Appl. Phys.*, **61**, 3295 (1987).
[32] M. Middleton, H. Place, R.D. Willett. *J. Am. Chem. Soc.*, **110**, 8639 (1988).
[33] R.D. Willett. *Acta Crystallogr.*, **C46**, 565 (1990).
[34] B. Kundys, A. Lappas, M. Viret, V. Kapustianyk, V. Rudyk, S. Semak, C. Simon, I. Bakaimi. *Phys. Rev. B*, **81**, 224434 (2010).
[35] A.O. Polyakov, A.H. Arkenbout, J. Baas, G.R. Blake, A. Meetsma, A. Caretta, P.H.M. van Loosdrecht, T.T.M. Palstra. *Chem. Mater.*, **24**, 133 (2012).
[36] R.D. Willett. *J. Chem. Phys.*, **44**, 39 (1966).
[37] L.P. Battaglia, A. Bonamartini Corradi, G. Marcotrigiano, L. Menabue, G.C. Pellacani. *Inorg. Chem.*, **19**, 125 (1980).
[38] L.P. Battaglia, A.B. Corradi, U. Geiser, R.D. Willett, A. Motori, F. Sandrolini, L. Antolini, T. Manfredini, L. Menabue, G.C. Pellacani. *J. Chem. Soc., Dalton Trans.*, 265 (1988).
[39] R.D. Willett, B. Twamley, W. Montfrooij, G.E. Granroth, S.E. Nagler, D.W. Hall, J.H. Park, B.C. Watson, M.W. Meisel, D.R. Talham. *Inorg. Chem.*, **45**, 7689 (2006).
[40] L. Brammer, J.K. Swearingen, E.A. Bruton, P. Sherwood. *Proc. Natl. Acad. Sci, USA*, **99**, 4956 (2002).
[41] J. Giantsidis, C. Galeriu, C.P. Landee, M.M. Turnbull. *J. Coord. Chem.*, **55**, 795 (2002).
[42] J. Qian, M.-J. Xie, L. Feng, J.-L. Tian, J. Shang, Y. Zhang, S.-P. Yan. *J. Coord. Chem.*, **63**, 2239 (2010).
[43] S. Jin, D. Wang. *J. Coord. Chem.*, **65**, 3188 (2012).
[44] W. Zhang, Y. Cai, R.-G. Xiong, H. Yoshikawa, K. Awaga. *Angew. Chem. Int. Ed.*, **49**, 6608 (2010).
[45] W. Zhang, H.-Y. Ye, R. Graf, H.W. Spiess, Y.-F. Yao, R.-Q. Zhu, R.-G. Xiong. *J. Am. Chem. Soc.*, **135**, 5230 (2013).
[46] W. Zhang, R.-J. Xu. *Sci. China Chem.*, **55**, 201 (2012).
[47] Y. Zhang, W. Zhang, S.-H. Li, Q. Ye, H.-L. Cai, F. Deng, R.-G. Xiong, S.D. Huang. *J. Am. Chem. Soc.*, **134**, 11044 (2012).
[48] A.J. Moulson, J.M. Herbert. *Electroceramics*, Wiley, Chichester (2003).
[49] L.-Z. Chen, J. Zou, Y.-M. Gao, S. Wan, M.-N. Huang. *J. Coord. Chem.*, **64**, 715 (2011).
[50] Th. Hahn (Ed). *Acta Cryst.*, **A51**, 592 (1995).